2007.

- "Inter-crystal identification for a depth-sensitive detector using support vector machine for small animal PET." Nucl. Instrum. & Methods A, 571, pp.243-246, 2007.
- "Detector normalization and scatter correction for the jPET-D4: A 4-layer depth-of-interaction PET scanner." Nucl. Instrum. & Methods A, 571, pp.231-234, 2007.
- "Annihilation photon acollinearity in PET : volunteer and phantom FDG studies." Phys. Med. Biol., 52, (1), pp.5249-5261, 2007.
- "Application of accelerators for the research and development of scintillators." Rev. Sci. Instr., 78, pp.083303 1-7, 2007.
- "Spatial resolution evaluation with a pair of two four-layer DOI detectors for small animal PET scanner: jPET-RD." Nucl. Instrum. & Methods A, 584, pp.212-218, 2008.
- "Performance evaluation for 120 four-layer DOI block detectors of the jPET-D4." Radiol. Phys. Technol., 1, pp.75-82, 2007.
- "A proposal of an open PET geometry." Phys. Med. Biol., *in press*.
- "Simplified simulation of four-layer depth of interaction detector for PET." Radiol. Phys. Technol., 1, pp.106-114, 2007.

2. 学会発表

- 「デンドリマーを用いたMRI用機能分子造影剤の開発に関する基礎的検討」（日本薬学会第126年会、2006年3月、仙台）
- 「低酸素特異的安定化タンパク質を利用した新規低酸素イメージング剤の開発に関する基礎的検討」（第45回日本核医学会総会、2005年11月、東京）
- 「マトリックスメタロプロテアーゼ－２を標的とする新規腫瘍診断用ペプチド放射性医薬品の開発」（第45回日本核医学会総会、2005年11月、東京）
- 「腫瘍及び炎症組織における^{3}H-FLTの集積」（第45回日本核医学会総会、2005年11月、東京）
- "Optical Imaging of HIF-1 activity in malignant solid tumors for evaluation of cancer therapies" (Forth Annual Meeting,Cologne, Germany, Sep, 2005)
- "The jPET-D4: Transaxial imaging performance of a novel 4-layer depth-of-interaction." (The 4th Japan-Korea Joint Meeeting on Medical Physics and the 5th Asia-Oceania Congress of Medical Physics, Kyoto, Sept.-Oct., 2005)
- "Four-layer depth-of-interaction detectors for the jPET-D4." (The 4th Japan-Korea Joint Meeeting on Medical Physics and the 5th Asia-Oceania Congress of Medical Physics, Kyoto, Sept.-Oct., 2005)
- "DOI detection capability of 3D crystal array standing over two PMTs." (The 4th Japan-Korea Joint Meeeting on Medical Physics and the 5th Asia-Oceania Congress of Medical Physics, Kyoto, Sept.-Oct., 2005)

- "8-layer depth-of-interaction encoding of 3-dimensional crystal array."
  (The 4th Japan-Korea Joint Meeeting on Medical Physics and the 5th Asia-Oceania Congress of Medical Physics, Kyoto, Sept.-Oct., 2005)
- "Resolution measurements of a four-layer DOI prototype detector for jPET-RD."
  (The 4th Japan-Korea Joint Meeeting on Medical Physics and the 5th Asia-Oceania Congress of Medical Physics, Kyoto, Sept.-Oct., 2005)
- "Calibration and evaluation of DOI detector for jPET-D4."
  (The 4th Japan-Korea Joint Meeeting on Medical Physics and the 5th Asia-Oceania Congress of Medical Physics, Kyoto, Sept.-Oct., 2005)
- "Accuracy measurement with a high-precision solid marker for PET head motion correction."
  (The 4th Japan-Korea Joint Meeeting on Medical Physics and the 5th Asia-Oceania Congress of Medical Physics, Kyoto, Sept.-Oct., 2005)
- "Low-dimensional semiconducting materials in developing ultra-fast scintillators."
  (The 4th Japan-Korea Joint Meeeting on Medical Physics and the 5th Asia-Oceania Congress of Medical Physics, Kyoto, Sept.-Oct., 2005)
- "Feasibility study on a noninvasive measurement system for boron concentration."
  (The 4th Japan-Korea Joint Meeeting on Medical Physics and the 5th Asia-Oceania Congress of Medical Physics, Kyoto, Sept.-Oct., 2005)
- "3D animations for medical physics education and learning."
  (The 4th Japan-Korea Joint Meeeting on Medical Physics and the 5th Asia-Oceania Congress of Medical Physics, Kyoto, Sept.-Oct., 2005)
- "A 12-channel CMOS preamplifier-shaper-discriminator ASIC for APD and gas counters."
  (IEEE Nuc. Sci. Sympo. & Med. Imag. Conf. 2005)
- "Quantum confinement effects in semiconducting scintillators."
  (IEEE Nuc. Sci. Sympo. & Med. Imag. Conf. 2005)
- "8-layer depth-of-interaction encoding of 3-dimensional crystal array."
  (IEEE Nuc. Sci. Sympo. & Med. Imag. Conf. 2005)
- "Measurement of 32x8x4 LYSO crystal responses of DOI detector for jPET-RD."
  (IEEE Nuc. Sci. Sympo. & Med. Imag. Conf. 2005)
- "DOI detection capability of 3D crystal array standing over two PMTs."
  (IEEE Nuc. Sci. Sympo. & Med. Imag. Conf. 2005)
- "Motion correction for jPET-D4: improvement of measurement accuracy with a solid marker."
  (IEEE Nuc. Sci. Sympo. & Med. Imag. Conf. 2005)
- "Event-by-event random and scatter estimator based on support vector machine using multi-anode outputs."
  (IEEE Nuc. Sci. Sympo. & Med. Imag. Conf. 2005)
- "The jPET-D4: imaging performance of the

4-layer depth-of-interaction PET scanner." (IEEE Nuc. Sci. Sympo. & Med. Imag. Conf. 2005)

・"The jPET-D4: simple and reliable construction method for 4-layer DOI crystal blocks." (IEEE Nuc. Sci. Sympo. & Med. Imag. Conf. 2005)

・"The jPET-D4: calibration and acquisition system of the 4-layer DOI-PET scanner." (IEEE Nuc. Sci. Sympo. & Med. Imag. Conf. 2005)

・「低酸素特異的安定化タンパク質を母体とした新規低酸素核医学イメージング剤の開発に関する基礎的検討」（第1回日本分子イメージング学会総会、2006年5月、京都）

・「がんの悪性度診断を目的としたMRI用デンドリマー造影剤の開発に関する基礎的検討」（第16回金属の関与する生体関連反応シンポジウム（SRM2006）、2006年6月、東京）

・「11C-methionine(MET)の腫瘍・肉芽腫への集積性の違い：18F-FDG及び18F-FLTとの比較」（第46回日本核医学会総会、2006年11月、鹿児島）

・「低酸素特異的安定化タンパク質を母体とした低酸素核医学イメージング剤の開発に関する基礎的検討；担癌マウスにおける体内挙動の評価」（日本薬学会第127年会、2007年3月、富山）

・「腫瘍低酸素イメージングを目的としたタンパク質放射性薬剤の細胞内移行性向上を目指した膜透過ペプチドの検討」（日本薬学会第127年会、2007年3月、富山）

・「HIF-1を利用したイメージング・ターゲティング」（BiomarkerとDDS：ナノ技術の多元と諸相、2007年2月15日、神戸）

・「HIF-1を利用した腫瘍内低酸素がん細胞のイメージング・ターゲティング」（第9回がん治療増感研究シンポジウム、2007年2月10～11日、奈良）

・「HIF-1を利用した低酸細胞のイメージング・ターゲティング」（第9回日本組織工学会、2006年９月７日～８日、京都）

・「すい臓がん同所移植モデルを用いた低酸素がん細胞のイメージングとターゲティング」（第10回がん分子標的治療研究会総会、2006年6月15日～16日、東京）

・「HIF-1を利用した腫瘍内低酸素がん細胞のイメージング・ターゲティング」（第３回日本癌学会カンファレンス、2006年3月9日～11日、長野県蓼科）

・「ドップラーシフトを利用した生体PETの角度揺動測定」（第43回アイソトープ・放射線研究発表会、2006年）

・"Inter-crystal scatter identification for a depth-sensitive detector using support vector machine for small animal PET." (Proc. of EuroMedIm2006, 1st European Conf. on Melecular Imaging Technology, Marseille, France, 2006)

・"Detector normalization and scatter correction for the jPET-D4: a 4-layer depth-of-interaction PET scanner." (Proc. of EuroMedIm2006, 1st European Conf. on Melecular Imaging Technology, Marseille, France, 2006)

- "Development of depth-of-interaction (DOI) detector for PET and prototype PET scanner."
  (Proc. of the six Japan-France workshop on radiobiology and isotopic imaging, June 19-22, 2006, CEA)
- "Limit of spatial resolution in FDG-PET due to annihilation photon non-collinearity."
  (IFMBE Proc. Vol. 14, Proc. of World Congress on Medical Physics and Biomedical Engineering 2006, Seol)
- "Recent advantages in PET and the new jPET-D4 system."
  (IFMBE Proc. Vol. 14, Proc. of World Congress on Medical Physics and Biomedical Engineering 2006, Seol)
- "3D image reconstruction with accurate system modeling for the jPET-D4."
  (IFMBE Proc. Vol. 14, Proc. of World Congress on Medical Physics and Biomedical Engineering 2006, Seol)
- "Performance evaluation of jPET-RD detector composed of 32 x 32 x 4 LYSO."
  (IFMBE Proc. Vol. 14, Proc. of World Congress on Medical Physics and Biomedical Engineering 2006, Seol)
- "Inter-crystal scatter identification for a depth-sensitive detector using multi-anode outputs."
  (2006 IEEE Nuc. Sci. Sympo. & Med. Imag.)
- "A healthy volunteer FDG-PET study on the limit of the spatial resolution due to annihilation radiation non-collinearity."
  (2006 IEEE Nuc. Sci. Sympo. & Med. Imag.)
- "Comparison of nonlinear position estimators for continuous scintillator detectors in PET."
  (2006 IEEE Nuc. Sci. Sympo. & Med. Imag.)
- "The jPET-D4: Performance evaluation of four-layer DOI-PET scanner using the NEMA NU2-2001 standard."
  (2006 IEEE Nuc. Sci. Sympo. & Med. Imag.)
- "Monte Carlo simulation study on detector arrangement for a small bore DOI-PET scanner: jPET-RD."
  (2006 IEEE Nuc. Sci. Sympo. & Med. Imag.)
- "Spatial resolution measured by a prototype system of two 4-layer DOI detectors for jPET-RD."
  (2006 IEEE Nuc. Sci. Sympo. & Med. Imag.)
- "Optimization of crystal arrangement on 8-Layer DOI PET detector."
  (2006 IEEE Nuc. Sci. Sympo. & Med. Imag.)
- "First human brain images of the jPET-D4 using 3D OS-EM with a pre-computed system matrix."
  (2006 IEEE Nuc. Sci. Sympo. & Med. Imag.)
- "Study of statistical and non-statistical components of enery resolution for position sensitive beta camera."
  (2006 IEEE Nuc. Sci. Sympo. & Med. Imag.)
- "Evaluation of annihilation radiation non-collinearity in positron emission tomography by measuring the Doppler effect."
  (Proc. of the 20th Workshop on Radiation Detectors and Their Uses, KEK

Proceedings 2006-7, Nov., 2006)

・「低酸素特異的安定化タンパク質を用いた担癌マウスでのイメージングの検討；担癌マウスにおける体内挙動の評価」
（日本分子イメージング学会第2回総会・学術集会、2007年6月、福井）

・「細胞の増殖能の評価及び腫瘍と肉芽腫の鑑別診断における^{11}C-メチオニンの有用性：^{18}F-FDGとの比較」
（日本分子イメージング学会第2回総会・学術集会、2007年6月、福井）

・「^{3}H-FLTによる癌の分子標的療法の早期治療効果評価：担がんマウスにおける投与量依存性の検討」
（第47回日本核医学会総会、2007年11月、仙台）

・「細胞の増殖能評価、腫瘍－肉芽腫の鑑別診断における^{11}C-methionineと^{18}F-FDGの比較」
（第47回日本核医学会総会、2007年11月、仙台）

・「塵肺合併肺癌の検出におけるFDG－PET後期追加の意義の検討」
（第47回日本核医学会総会、2007年11月、仙台）

・「酸素依存的分解タンパク質を利用した低酸素イメージング剤の開発；担癌マウスでのプレターゲット法の評価」
（第47回日本核医学会総会、2007年11月、仙台）

・「酸素依存的分解タンパク質を母体とする腫瘍低酸素領域の核医学イメージング剤の開発」
（第5回がんとハイポキシア研究会、2007年12月、柏）

・「光イメージングを用いた生体応答の可視化と治療薬・診断薬の開発」
（第24回日本毒性病理学会総会「画像イメージングと毒性病理学の接点」、2008年2月、名古屋）

・「腫瘍内低酸素がん細胞のイメージング・ターゲティング」
（日本癌学会シンポジウム「がんの光イメージング」、2007年10月、横浜）

・"A new strategy to target HIF-1."
(13th International congress of Radiation Research, July, 2007, San Francisco)

・"^{18}F-FLT but not ^{18}F-FDG can early and dose-dependently detect antiproliferative responses of human tumor xenograft to epidermal growth factor receptor targeting with a tyrosine kinase inhibitor, gefitinib."
(54th Annual Meeting of the Society of Nuclear Medicine. Jun., 2007, Washington DC)

・"Complementary role of methionine-PET and FDG-PET for differentiation between benign lesions and lung cancer in patients with pneumoconiosis."
(54th Annual Meeting of the Society of Nuclear Medicine. Jun., 2007, Washington DC)

・"Usefulness of ^{11}C-methionine in evaluating cellular proliferation and differential diagnosis of tumor and granuloma: An experimental study in comparison with ^{18}F-FDG."
(54th Annual Meeting of the Society of Nuclear Medicine. Jun., 2007, Washington DC)

・"Development of a hypoxia-targeting probe based on the mechanism of oxygen-dependent degradation of hypoxia-inducible factor-1α."
(54th Annual Meeting of the Society of

Nuclear Medicine. Jun., 2007, Washington DC)

- "Membrane type-1 matrix metalloproteinase (MT1-MMP), a potential target for radioimmuno-detection and therapy of malignant tumors: Evaluation in experimental rat models."
  (Joint Molecular Imaging Conference. Sep., 2007, Providence)
- "Development of radiolabeled hypoxia imaging agent based on the mechanism of oxygen-dependent degradation of hypoxia-inducible factor-1 alpha."
  (Seventh Japan-China Joint Seminar on Radio-pharmaceutical Chemistry. Sep., 2007, Kyoto)
- "Development of hypoxia imaging probe utilizing oxygen-dependent degradation domain of hypoxia-inducible factor-1a."
  (The Hypoxia Workshop in Hokkaido. Nov., 2007, Sapporo)
- "Clinical value of image fusion of MR with PET images in patients with head and neck cancer."
  (54th Annual Meeting of the Society of Nuclear Medicine. Jun., 2007, Washington DC)
- "Implementation of 3D image reconstruction with a pre-computed system matrix for the jPET-D4."
  (Proc. 9th Intern. Meeting on Fully Three-Dimensional Image Reconst. in Radiol. and Nucl. med., July 8-13, 2007, Lindau, Germany)
- "3D PET image reconstructin with on-the-fly system matrix generation accelerated by utilizing shift and symmetry properties."
  (Proc. 9th Intern. Meeting on Fully Three-Dimensional Image Reconst. in Radiol. and Nucl. med., July 8-13, 2007, Lindau, Germany)
- "Improvement of PET image quality using DOI and TOF information."
  (Proc. 9th Intern. Meeting on Fully Three-Dimensional Image Reconst. in Radiol. and Nucl. med., July 8-13, 2007, Lindau, Germany)
- "Novel Front-End Pulse Processing Scheme for PET System Based on Pulse Width Modulation and Pulse Train Method."
  (2007 IEEE Nuc. Sci. Sympo. & Med. Imag. Conf. Record., NM2-7, 2007)
- "A DOI-Dependent Extended Energy Window Method to Control Balance of Scatter and True Events."
  (2007 IEEE Nuc. Sci. Sympo. & Med. Imag. Conf. Record., M03-8)
- "DOI Encoding on the PET Detector Using 2 X 2 PMT Array."
  (2007 IEEE Nuc. Sci. Sympo. & Med. Imag. Conf. Record., M13-157)
- "Parallel Implementation of 3-D Dynamic Iterative Reconstruction with Intra-node Image Update for the jPET-D4."
  (2007 IEEE Nuc. Sci. Sympo. & Med. Imag. Conf. Record., M13-221)
- "Preliminary Study of a DOI-PET Detector with Optical Imaging Capability."
  (2007 IEEE Nuc. Sci. Sympo. & Med. Imag. Conf. Record., M18-22)
- "System Modeling of Small Bore DOI-PET Scanners for Fast and Accurate 3D Image Reconstruction."
  (2007 IEEE Nuc. Sci. Sympo. & Med. Imag. Conf. Record., M18-242)
- "Timing Resolution Improved by DOI

Information in a Four-Layer LYSO PET Detector."
(2007 IEEE Nuc. Sci. Sympo. & Med. Imag. Conf. Record., M19-7)

・"Four-Layer DOI Detector with a Multi Pixel APD by Light Sharing Method for Small Animal PET."
(2007 IEEE Nuc. Sci. Sympo. & Med. Imag. Conf. Record., M19-11)

・"A Proposal of Open PET Geometies."
(2007 IEEE Nucl. Sci. & Med. Imag. Conf. Record., M19-19)

H．知的財産権の出願・登録状況

1．特許出願

・近藤科江、原田浩、平岡真寛、山田秀一：病態の状態をリアルタイムで観察可能なモデル動物とそれを可能にする遺伝子構築物及びその使用
2006年3月10日出願
国際出願番号PCT/JP2006/304701

・稲玉直子、村山秀雄、 澁谷憲悟、北村圭司、石橋浩之：放射線位置検出方法及び装置
平成17年9月28日出願、
出願番号　特願2005-282866

・北村圭司、吉田英治、村山秀雄、木村裕一：放射線同時計数処理方法、放射線同時計数処理プログラム、および放射線同時計数処理記憶媒体並びに放射線同時計数装置およびそれを用いた核医学診断装置
平成17年10月20日出願
出願番号　特願2005-305944

・北村圭司、吉澤昌由加、稲玉直子、村山秀雄：マンモグラフィ装置
平成18年3月31日出願
出願番号：特願2006-097320

・清水成宜、石橋浩之、村山秀雄、津田倫明、稲玉直子、山谷泰賀：放射線検出器
平成18年4月25日出願
出願番号：特願2006-120680

・澁谷憲悟、津田倫明、錦戸文彦、稲玉直子、吉田英治、山谷泰賀、村山秀雄：陽電子放射断層撮像装置及び放射線検出器
平成18年8月25日出願
出願番号：特願2006-229376

・オーストラリア2002304163
Polypeptide unstablizing protein in cells under aerobic conditions and DNA encoding the same.
発明者：平岡真寛・近藤科江・原田浩
登録日：2007年8月30日
出願人：平岡真寛・近藤科江・ポーラ化成工業株式会社

・Shibuya, K., Tsuda, T., Nishikido, F., Inadama, N., Yoshida, E., Yamaya, T., Murayama, H. : Positron emission tomography scanner and radiation detector, January 31, 2007. 出願番号 PCT/JP2006/326357. （米国特許庁）

・長谷川智之、村山秀雄、山谷泰賀：被験体の３次元的位置及び向き測定装置
平成19年3月6日出願
出願番号　特願2007-55044号

・佐藤泰、村山秀雄、山田崇裕：放射能絶対測定方法、放射線検出器集合体の検出効率決定方法、及び、放射線測定装置の校正方法
平成19年3月29日出願
出願番号　特願2007-87317号

・山谷泰賀、村山秀雄、吉田英治：断層撮影装置の画像再構成方法、故障診断方法、断層撮影装置、及び、システムマトリクスの管理プログラム

平成19年3月29日出願
出願番号　特願2007-87480号

・山谷泰賀、村山秀雄、吉田英治：断層撮影装置の画像再構成方法、故障診断方法、断層撮影装置、及び、システムマトリクスの管理プログラム
平成19年3月30日国際出願
国際出願番号 PCT/JP2007/057229

・山谷泰賀、村山秀雄、簑原伸一：PET装置、及び、その画像再構成方法
平成19年4月17日国際出願
国際出願番号PCT/JP2007/058361

・吉田英治、澁谷憲悟、山谷泰賀、村山秀雄：エネルギーと位置情報を利用した放射線検出方法及び装置
平成19年4月23日出願
出願番号　特願2007-112925号

・稲玉直子、村山秀雄、澁谷憲悟、錦戸文彦、大井淳一、津田倫明：放射線位置検出器
平成19年8月28日出願
出願番号　特願2007-221441号

2．特許登録

・村山秀雄、石橋浩之、山下貴司、内田博、大村知秀：放射線入射位置３次元検出器の発行位置特定方法,
平成17年7月8日登録
特許第3697340号

・Murayama, H., Inadama, N., Kitamura, K., Yamashita, T.: Radiation three-dimensional position detector,
August 8, 2006.
Patent No.: US 7,087,905 B2（米国特許庁）

・Sumiya, K., Ishibashi, H., Murayama, H., Inadama, N., Yamashita, T., Omura, T. : Depth of interaction with uniform pulse-height,
August 15, 2006.
Patent No.: US 7,091,490 B2（米国特許庁）

・山本誠一，村山秀雄：強磁場内作動型放射線位置検出器
平成19年5月11日登録
特許第3950964号

研究成果の刊行に関する一覧表

書籍

著者氏名	論文タイトル名	書籍全体の編集者名	書　籍　名	出版社名	出版地	出版年	ページ
近藤科江 平岡真寛	小動物を用いた光イメージング研究の現状	宇理須恒雄	ナノメデイシンの基礎と最先端（仮題）	オーム社	日本	印刷中	

雑誌

発表者氏名	論文タイトル名	発表誌名	巻号	ページ	出版年
Kuge Y, Katada Y, Shimonaka S, Temma T, Kimura H, Kiyono Y, Yokota C, Minematsu K, Seki K, Tamaki N, Ohkura K, Saji H.	Synthesis and evaluation of radioiodinated cyclooxygenase-2 inhibitors as potential SPECT tracers for cyclooxygenase-2 expression.	Nucl Med Biol	33(1)	21-27	2006
Ogawa K, Mukai T, Arano Y, Ono M, Hanaoka H, Ishino S, Hashimoto K, Nishimura H, Saji H.	Development of a rhenium-186-labeled MAG3-conjugated bisphosphonate for the palliation of metastatic bone pain based on the concept of bifunctional radiopharmaceuticals.	Bioconjugate Chem	16(4)	751-757	2005
Obata A, Kasamatsu S, Lewis JS, Furukawa T, Takamatsu S, Toyohara J, Asai T, Welch MJ, Adams SG, Saji H, Yonekura Y, Fujibayashi Y.	Basic characterization of ^{64}Cu-ATSM as a radiotherapy agent.	Nucl Med Biol	32(1)	21-28	2005
Takei T, Kuge Y, Zhao S, 他	Enhanced apoptotic reaction correlates with suppressed tumor glucose utilization after cytotoxic chemotherapy: use of ^{99m}Tc-Annexin V, ^{18}F-FDG, and histologic evaluation.	J Nucl Med	46(5)	794-799	2005

Zhao S, Kuge Y, Mochizuki T, 他	Biologic correlates of intratumoral heterogeneity in 18F-FDG distribution with regional expression of glucose transporters and hexokinase-II in experimental tumor.	J Nucl Med	46(4)	675-682	2005
Liu J, Qu R, Ogura M, Shibata T, Harada H, Hiraoka M.	Real-time imaging of hypoxia-inducible factor-1 activity in tumor xenografts	J Radiat Res (Tokyo)	46	93-102	2005
Harada H, Kizaka-Kondoh S, Hiraoka M.	Optical imaging of tumor hypoxia and evaluation of efficacy of a hypoxia-targeting drug in living animals.	Mol Imaging	4	182-93	2005
Ogura M, Shibata T, Yi J, Liu J, Qu R, Harada H, Hiraoka M.	A tumor-specific gene therapy strategy targeting dysregulation of the VHL/HIF pathway in renal cell carcinomas	Cancer Sci	96	288-94	2005
Harada H, Kizaka-Kondoh S, Hiraoka M.	Antitumor protein therapy; application of the protein transduction domain to the development of a protein drug for cancer treatment.	Breast Cancer	13	16-26	2006
Okada T, Miki Y, Fushimi Y, Hanakawa T, Kanagaki M, Yamamoto A, Urayama S, Fukushima H, et al.	Diffusion-tensor fiber tractography: intraindividual comparison of 3.0-T and 1.5T MR imaging.	Radiology	238	668-678	2006
Kikuta K, Takagi Y, Nozaki K, Hanakawa T, Okada T, Miki Y, Fushimi Y, Fukuyama H, Hashimoto N.	Early experiment with 3-T magnetic resonance tractography in the surgery of cerebral arteriovenous malformations in and around the visual pathway.	Neurosurgery	58	331-337	2006

近藤科江、 原田浩、 平岡真寛	革新的診断・治療へのアプローチ; 膜透過性・標的特異性を有する融合タンパク質を用いたイメージング、ターゲティング	BioClinica	20(1)	53-58	2005
近藤科江、 平岡真寛、 原田浩	がん治療における HIF-1とTumor Hypoxia	Cancer Frontier	7	77-86	2005
近藤科江、 原田浩、 平岡真寛	『低酸素がん細胞』を標的としたがんのイメージング・ターゲティング	バイオテクノロジージャーナル	6 (2)	234-237	2006
Ogawa K, Mukai T, Asano D,Kawashima H, Kinuya S, Shiba K,Hashimoto K, Mori H, Saji H.	Therapeutic effects of a186Re-complex-conjugated bisphosphonate for the palliation of metastatic bone pain in an animal model.	J Nucl Med	48(1)	122-7	2007
Ogawa K, Mukai T, Inoue Y,Ono M, Saji H.	Development of a novel 99mTc-chelate-conjugated bisphosphonate with high affinity for bone as a bone scintigraphic agent.	J Nucl Med	47(12)	2042-7	2006
Ogawa K, Mukai T, Arano Y,Otaka A, Ueda M, Uehara T, Magata Y, Hashimoto K, Saji H.	Rhemium-186-Monoaminemonoamide-dithiol-conjugated bisphosphonate derivatives for bone pain palliation.	Nucl Med Biol	33(4)	513-20	2006
Hanaoka H, Mukai T, Tamamura H, Mori T, Ishino S, Ogawa K, Iida Y, Doi R, Fujii N, Saji H.	Development of a 111In-labeled peptide derivative targeting a chemokine receptor, CXCR4, for imaging tumors.	Nucl Med Biol	33(4)	489-94	2006
Ohkura K, Yamaguchi T, Nishijima K, Kuge Y, Seki K	Photochemical synthesis of polycyclic pyrimidines through the acid catalyzed cycloaddition of 6-chloro-1-methyluracil to methyl substituted benzenes.	Heterocycles	70	501-508	2006

Ohkura K, Nishijima K, Sanoki K, Kuge Y,Tamaki N, Seki K.	A new convenient method for the synthesis of [2-^{11}C]thymine utilizing [^{11}C]phosgene.	Tetrahedron Letters	47	5321-5323	2006
Tanaka S, Kizaka-Kondoh S, HaradaH, Hiraoka M.	Development of a novel fluorescent imaging probe for tumor hypoxia by use of a fusion protein with oxygen-dependent degradation domain of HIF-1α.	Genetically Engineered and Optical Probes for Biomedical Applications IV, Proceedings of SPIE	6449	64490Y	2007
Harada H, Kizaka-Kondoh S, Hiraoka M.	Mechanism of hypoxia-specific cytotoxicity of procaspase-3 fused with a VHL-mediated protein destruction motif of HIF-1α containing Pro564.	FEBS Lett	580	5718-5722	2006
Kageyama Y, Sugiyama H, Ayame H, Iwai A, Fujii Y, L Eric Huang, Kizaka-Kondoh S, Hiraoka M, Kihara K.	Suppression of VEGF transcription in renal cell carcinoma cells by pyrrole-imidazole hairpin polyamides targeting the hypoxia responsive element.	Acta Oncologica	45(3)	317-324	2006
Oka S, Masutani H, Liu W, Horita H, Wang D, Kizaka-Kondoh S, Yodoi J.	Thioredoxin-binding protein-2 (TBP-2)-like inducible membrane protein (TLIMP) is a novel Vitamin D3- and PPAR-γ ligand target protein that regulates PPAR-γ signaling.	Endocrinology	147 (2)	733-743	2006
近藤科江、平岡眞寛	低酸素を標的とした生体イメージング分子プローブの開発	未来医学	21	32-37	2006
田中正太郎、近藤科江	蛍光の生体イメージングへの応用	Bioclinica	21(11)	992-998	2006
近藤科江、原田浩、田中正太郎、平岡眞寛	HIF-1を利用した腫瘍内低酸素がん細胞のイメージング・ターゲティング 1	放射線科学	49 (11)	399-404	2006
近藤科江、原田浩、田中正太郎、平岡眞寛	HIF-1を利用した腫瘍内低酸素がん細胞のイメージング・ターゲティング 2	放射線科学	49 (12)	436-441	2006

Hanaoka H, Mukai T, Habashita S, Asano D, Ogawa K, Kuroda Y, Akizawa H, Iida Y, Endo K, Saga T, Saji H.	Chemical design of a radiolabeled gelatinase inhibitor peptide for the imaging of gelatinase activity in tumors.	Nucl Med Biol	34(5)	503-10	2007
Zhao S, Kuge Y, Kohanawa M, Takahashi T, Zhao Y, Yi M, Kanegae K, Seki K, Tamaki N.	Usefulness of ^{11}C-Methionine for Differentiating Tumors from Granulomas in Experimental Rat Models: A Comparison with ^{18}F-FDG and ^{18}F-FLT.	J Nucl Med	49(1)	135-141	2008
Zhao S, Kuge Y, Kohanawa M, Takahashi T, Kawashima H, Temma T, Takei T, Zhao Y, Seki K, Tamaki N.	Extensive 18F-FDG Uptake and Its Modification with Corticosteroid in a Granuloma Rat Model: An Experimental Study for Differentiating Granuloma from Tumors.	Eur J Nucl Med Mol Imaging	34(12)	2096-105	2007
Kanegae K, Nakano I, Kimura K, Kaji H, Kuge Y, Shiga T, Zhao S, Okamoto S, Tamaki N.	Comparison of MET-PET and FDG-PET for differentiation between benign lesions and lung cancer in pneumoconiosis.	Ann Nucl Med	21(6)	331-337	2007
Seki K, Nishijima K, Kuge Y, Tamaki N, Wiebe LI, Ohkura K.	A novel and efficient synthesis of [2-^{11}C]5-fluorouracil for prognosis of cancer chemotherapy.	J Pharm Pharmaceut Sci	10(2)	181-185	2007
Kimura M, Takabuchi S, Tanaka T, Murata M, Nishi K, Oda S, Oda T, Kanai M, Fukuda K, Kizaka-Kondoh S, Adachi T, Takabayashi A, Semenza GL, Hirota K.	n-propyl gallate activates hypoxia-inducible factor 1 by modulating intracellular oxygen-sensing systems.	Biochemical J			in press
Tanisaka H, Kizaka-Kondoh S, Makino A, Tanaka S, Hiraoka M, Kimura, S.	Near-Infrared Fluorescent Labeled Peptosome for Application to Cancer Imaging.	Bioconjugate Chem	19(1)	109-117	2008

Tanabe K, Hirata N, Harada H, Hiraoka M, Nishimoto S.	Emission under hypoxia: one-electron reduction and fluorescence characteristics of an indolequinone-coumarin conjugate.	Chembiochem	9(3)	426-432	2008
Harada H, Kizaka-Kondoh S, Li G, Itasaka S, Shibuya K, Inoue M, Hiraoka M.	Significance of HIF-1-active cells in angiogenesis and radioresistance.	Oncogene	26(54)	7508-7516	2007
Harada H, Kizaka-Kondoh S, Itasaka S, Shibuya K, Morinibu A, Shinomiya K, Hiraoka M.	The combination of hypoxia-response enhancers and an oxygen-dependent proteolytic motif enables real-time imaging of absolute HIF-1 activity in tumor xenografts	Biochem Biophys Res Commun	360(4)	791-796	2007
Liu J, Harada H, Ogura M, Shibata T, Hiraoka M.	Adenovirus-mediated hypoxia-targeting cytosine deaminase gene therapy enhances radiotherapy in tumour xenografts.	Br J Cancer	96(12)	1871-1878	2007
Zeng L, Kizaka-Kondoh S, Itasaka S, Xie X, Inoue M, Tanimoto K, Shibuya K, Hiraoka M.	Hypoxia inducible factor-1 influences sensitivity to paclitaxel of human lung cancer cell lines under normoxic conditions.	Cancer Sci	98(9)	1394-1401	2007
Hiraga, T, Kizaka-Kondoh S, Hirota K, Hiraoka M, Yoneda T.	Hypoxia and hypoxia-inducible factor-1 expression enhance osteolytic bone metastases of breast cancer.	Cancer Res	67(9)	4157-4163	2007
Takaya S, Hashikawa K, Turkheimer FE, Mottram N, Deprez M, Ishizu K, Kawashima H, Akiyama H, Fukuyama H, Banati RB, Roncaroli F.	The lack of expression of the peripheral benzodiazepine receptor characterises microglial response in anaplastic astrocytomas.	J Neurooncol	85(1)	95-103	2007
久下裕司、上田真史、趙松吉、工藤喬、近藤科江、田中正太郎、玉木長良、平岡眞寛、佐治英郎	放射線治療を指向したPET/SPECTプローブの開発～低酸素イメージングを中心に～	癌の臨床	54(2)	105-108	2008

近藤科江、 田中正太郎、 冨本秀和	生体内バリアを回避する低酸素応答性人口たんぱく質の開発	血管医学			印刷中
神崎達也、牧野顕、木村俊作、近藤科江、平岡真寛、小関英一	新しいナノキャリア"ペプトソーム" 次世代DDSへの期待	化学と生物	45(11)	779-784	2007
近藤科江、 田中正太郎、 平岡真寛	「環境標的」としてのがんの微小環境	Medical Bio	4(7)	24-29	2007
近藤科江	日進月歩で進むイメージング技術の癌診断への応用	実験医学	25(17)	2770-2777	2007
近藤科江、 田中正太郎、 平岡真寛	腫瘍の悪性度を可視化する低酸素イメージング	実験医学	25(17)	2805-2812	2007
近藤科江、 田中正太郎	環境標的としての低酸素細胞の光イメージング	実験医学	25(14)	2144-2150	2007
木村俊作、 近藤科江、 平岡真寛	分子イメージングへ応用するナノキャリアの開発	化学	62(7)	34-37	2007
近藤科江、 平岡真寛	HIF-1を利用した腫瘍内低酸素がん細胞のイメージング	放射線生物研究	42(2)	162-173	2007
近藤科江、 平岡真寛	低酸素イメージング・発光イメージング	病理と臨床	25(6)	539-545	2007
近藤科江、 平岡真寛	HIF-1を利用した低酸素がん細胞のイメージング・ターゲティング	日本疾患モデル学会記録	23	43-50	2007
板坂聡、 原田浩、 近藤科江、 平岡真寛	新しい分子イメージングの活用 1.新しい治療法評価への分子イメージングの応用 2.放射線治療の分子イメージング	遺伝子医学MOOK	9	279-283	2007

Available online at www.sciencedirect.com
SCIENCE DIRECT
Nuclear Medicine and Biology 33 (2006) 21–27
NUCLEAR MEDICINE — AND — BIOLOGY
www.elsevier.com/locate/nucmedbio

Synthesis and evaluation of radioiodinated cyclooxygenase-2 inhibitors as potential SPECT tracers for cyclooxygenase-2 expression

Yuji Kuge[a,*], Yumiko Katada[a], Sayaka Shimonaka[a], Takashi Temma[a], Hiroyuki Kimura[a], Yasushi Kiyono[b], Chiaki Yokota[c], Kazuo Minematsu[d], Koh-ichi Seki[e], Nagara Tamaki[f], Kazue Ohkura[g], Hideo Saji[a]

[a]*Department of Patho-Functional Bioanalysis, Graduate School of Pharmaceutical Sciences, Kyoto University, Kyoto 606-8501, Japan*
[b]*Radioisotopes Research Laboratory, Kyoto University Hospital, Faculty of Medicine, Kyoto University, Kyoto 606-8507, Japan*
[c]*Cerebrovascular Laboratory, National Cardiovascular Center Research Institute, Osaka 565-8565, Japan*
[d]*Cerebrovascular Division, Department of Medicine, National Cardiovascular Center Research Institute, Osaka 565-8565, Japan*
[e]*Central Institute of Isotope Science, Hokkaido University, Hokkaido 060-8638, Japan*
[f]*Department of Nuclear Medicine, Graduate School of Medicine, Hokkaido University, Hokkaido 060-8638, Japan*
[g]*Department of Radiopharmaceutical Chemistry, Faculty of Pharmaceutical Sciences, Health Sciences University of Hokkaido, Hokkaido 061-0293, Japan*

Received 26 August 2005; received in revised form 30 September 2005; accepted 5 October 2005

Abstract

Although several COX-2 inhibitors have recently been radiolabeled, their potential for imaging COX-2 expression remains unclear. In particular, the sulfonamide moiety of COX-2 inhibitors may cause slow blood clearance of the radiotracer, due to its affinity for carbonic anhydrase (CA) in erythrocytes. Thus, we designed a methyl sulfone-type analogue, 5-(4-iodophenyl)-1-[4-(methylsulfonyl)phenyl]-3-trifluoromethyl-1*H*-pyrazole (IMTP). In this study, the potential of radioiodinated IMTP was assessed in comparison with a ^{125}I-labeled celecoxib analogue with a sulfonamide moiety (^{125}I-IATP).

Methods: The COX inhibitory potency was assessed by measuring COX-catalyzed oxidation by hydrogen peroxide. The biodistribution of ^{125}I-IMTP and ^{125}I-IATP was determined by the ex vivo tissue counting method in rats. Distribution of the labeled compounds to rat blood cells was measured.

Results: The COX-2 inhibitory potency of IMTP (IC_{50}=5.16 μM) and IATP (IC_{50}=8.20 μM) was higher than that of meloxicam (IC_{50}=29.0 μM) and comparable to that of SC-58125 (IC_{50}=1.36 μM). The IC_{50} ratios (COX-1/COX-2) indicated the high isoform selectivity of IMTP and IATP for COX-2. Significant levels of ^{125}I-IMTP and ^{125}I-IATP were observed in the kidneys and the brain (organs known to express COX-2). The blood clearance of ^{125}I-IMTP was much faster than that of ^{125}I-IATP. Distribution of ^{125}I-IATP to blood cells (88.0%) was markedly higher than that of ^{125}I-IMTP (18.1%), which was decreased by CA inhibitors.

Conclusions: Our results showed a high inhibitory potency and selectivity of IMTP for COX-2. The substitution of a sulfonamide moiety to a methyl sulfone moiety effectively improved the blood clearance of the compound, indicating the loss of the cross reactivity with CA in ^{125}I-IMTP. ^{123}I-IMTP may be a potential SPECT radiopharmaceutical for COX-2 expression.

Keywords: Cyclooxygenase-2 (COX-2); Inhibitor; Radioiodination; SPECT; Radiopharmaceutical

1. Introduction

Cyclooxygenases (COXs) catalyse the key rate-limiting step in the conversion of arachidonic acid into prostaglandins and thromboxanes. To date, at least 2 distinct isoforms of the COXs—a constitutive form (COX-1) and an inducible isoform (COX-2)—and several of their variants have been discovered [1]. COX-1 is constitutively expressed in most tissues and is responsible for maintaining homeostasis, whereas COX-2 is induced in response to inflammatory stimuli. Besides being associated with inflammation, COX-2 has been implicated in a number of pathological processes, including many human cancers, atherosclerosis, and cerebral and cardiac ischemia [2–5]. We also reported

* Corresponding author. Tel.: +81 75 753 4608; fax: +81 75 753 4568.
E-mail address: kuge@pharm.kyoto-u.ac.jp (Y. Kuge).

0969-8051/$ – see front matter © 2006 Elsevier Inc. All rights reserved.
doi:10.1016/j.nucmedbio.2005.10.004

the neuronal expression of COX-2 in rodent and primate models of cerebral ischemia [6–10].

Accordingly, the noninvasive imaging of COX-2 expression should help in understanding the pathophysiology of the diseases and contribute to the clinical use of COX-2 inhibitors [11]. In this regard, several COX-2 inhibitors were recently radiolabeled with F-18 and their potentials for positron emission tomography (PET) tracers were preliminarily evaluated [12–14]. The results for the potentials of these labeled compounds, however, are not necessarily consistent from one laboratory to another. In addition, the short half-life of ^{18}F may hamper the determination of the specific binding of the tracer to COX-2, because it is known that the COX-2 inhibitors show time-dependent inhibition of COX-2 [11]. The longer half-lives of single photon emission tomography (SPECT) nuclides, such as Tc-99m or I-123, may be more suitable for radiotracers to image COX-2. From these points of view, we intended to develop radioiodinated COX-2 inhibitors as SPECT tracers for imaging COX-2 expression.

As for SPECT tracers, Yang et al. [15] proposed a ^{99m}Tc-labeled celecoxib (celebrex) analogue as a potential tracer for COX-2 expression. Kabalka et al. [16] recently reported the radiosynthesis of a ^{123}I-labeled celecoxib analogue. However, the detailed characteristics of these tracers, including affinity and selectivity to COX-2, have not

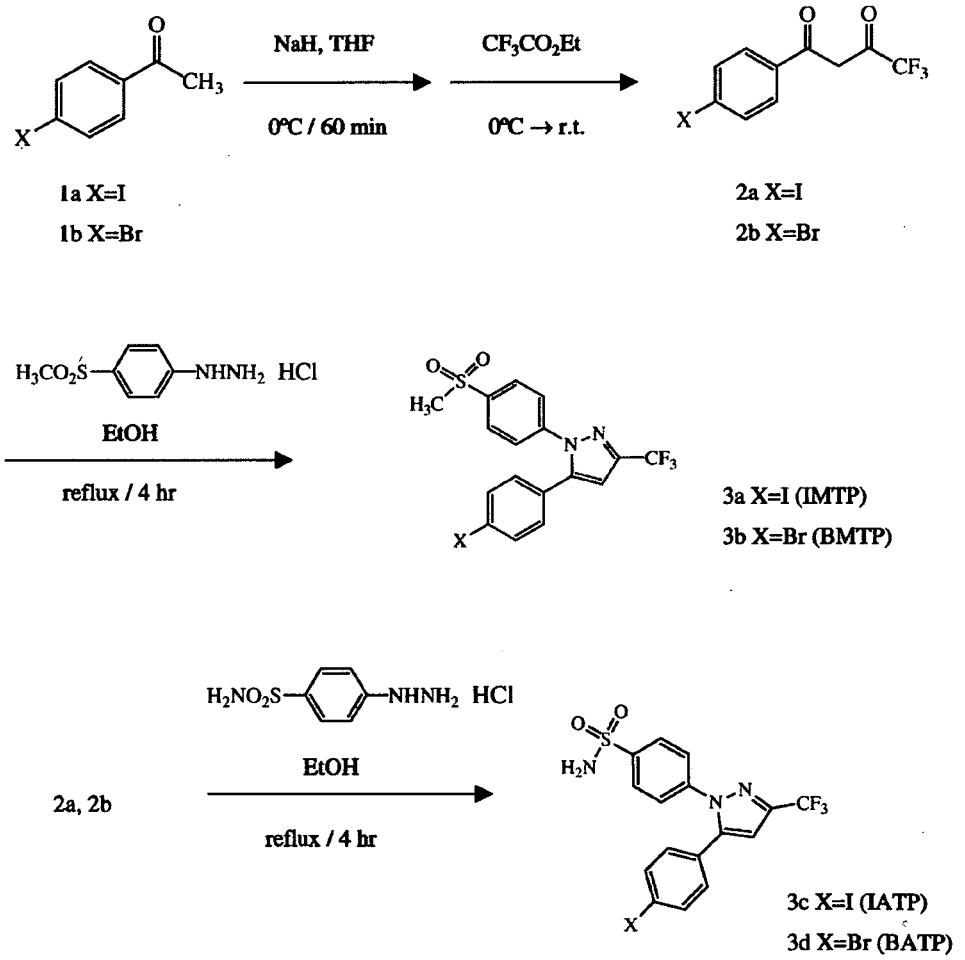

Fig. 1. Synthesis of IMTP (compound **3a**), BMTP (compound **3b**), IATP (compound **3c**) and BATP (compound **3d**).
Compound 1a, iodoacetophenone
Compound 1b, bromoacetophenone
Compound 2a, 4,4,4-trifluoro-1-(4-iodophenyl)-butane-1,3-dione
Compound 2b, 4,4,4-trifluoro-1-(4-bromophenyl)-butane-1,3-dione
Compound 3a, 5-(4-iodophenyl)-1-[4-(methylsulfonyl)phenyl]-3-trifluoromethyl-1H-pyrazole
Compound 3b, 5-(4-bromophenyl)-1-[4-(methylsulfonyl)phenyl]-3-trifluoromethyl-1H-pyrazole
Compound 3c, 5-(4-iodophenyl)-1-[4-(aminosulfonyl)phenyl]-3-trifluoromethyl-1H-pyrazole
Compound 3d, 5-(4-bromophenyl)-1-[4-(aminosulfonyl)phenyl]-3-trifluoromethyl-1H-pyrazole

been determined and their usefulness remains unclear. In particular, the sulfonamide moiety of celecoxib may cause slow blood clearance of the radiotracer, due to its affinity for carbonic anhydrase in erythrocytes [17,18].

Thus, we designed a methyl sulfone-type analogue, 5-(4-iodo-phenyl)-1-[4-(methylsulfonyl)phenyl]-3-trifluoromethyl-1*H*-pyrazole (IMTP), iodinated at position 4 of the 5-phenyl ring as a SPECT tracer for imaging COX-2 expression (Fig. 1). In this study, radioiodinated IMTP was synthesized, and its potential was assessed in comparison with a ^{125}I-labeled cerecoxib analogue with a sulfonamide moiety (^{125}I-IATP).

2. Materials and methods

2.1. General

Sodium ^{125}I-iodide (642.8 GBq/mg) was purchased from Perkin Elmer Life and Analytical Sciences (Boston, MA). All chemicals used were of reagent grade.

Proton nuclear magnetic resonance (^{1}H NMR) spectra were recorded on a JNM-EX 400 spectrometer (JEOL, Tokyo, Japan), and the chemical shifts were reported in parts per million (ppm) downfield from an internal tetramethylsilane standard. Fast atom bombardment (FAB) mass spectra were recorded with a JMS-HX/HX110A model spectrometer (JEOL).

2.2. Synthesis

2.2.1. 5-(4-Iodophenyl)-1-[4-(methylsulfonyl)phenyl]-3-trifluoromethyl-1H-pyrazole (IMTP)

IMTP was synthesized according to the procedure outlined in Fig. 1. To dry tetrahydrofuran (THF, 5 mL) were added NaH (19.5 mg, 0.49 mmol) and iodoacetophenone 1a (100 mg, 0.4 mmol). The mixture was stirred at 0°C for 60 min, and then ethyl trifluoroacetate (145 μL, 1.22 mmol) was added dropwise. After stirring at 0°C for 12 h and at room temperature for 12 h, the reaction mixture was acidified with 1N HCl and then neutralized with 1N NaOH. The reaction mixture was extracted with chloroform. The organic layer was washed with brine, dried over Na_2SO_4, filtered and concentrated in vacuo to give brownish oil. The crude product was purified by silica gel column chromatography (AcOEt/hexane/triethylamine= 1:6:0.01) to give 2a as brownish oil in a yield of 35%. ^{1}H NMR ($CDCl_3$) δ, 7.71 (d, J=7.3 Hz, 2H), 7.51 (d, J=7.6 Hz, 2H), 6.30 (s, 1H).

Compound 2a (45.7 mg, 0.134 mmol) and 4-methylsulfonyl-phenylhydrazine hydrochloride (29.8 mg, 0.134 mmol) were dissolved in ethanol (3 ml) and heated under reflux for 4 h. The mixture was allowed to cool before concentration. The crude product was purified by silica gel flash column chromatography (AcOEt/hexane=1:2) to give IMTP 3a as a colorless solid in a yield of 51%. ^{1}H NMR ($CDCl_3$) δ, 7.97 (d, J=8.8 Hz, 2H), 7.74 (d, J=8.5 Hz, 2H), 7.53 (d, J=8.8 Hz, 2H), 6.97 (d, J=8.3 Hz, 2H), 6.79 (s, 1H), 3.08 (s, 3H). FAB-MS calcd for $C_{17}H_{12}IF_3N_2O_2S$ [MH^+]: m/z 493, found 493.

2.2.2. 5-(4-Bromophenyl)-1-[4-(methylsulfonyl)phenyl]-3-trifluoromethyl-1H-pyrazole (BMTP)

BMTP was synthesized in the same manner as IMTP, using bromoacetophenone 1b (100 mg, 0.5 mmol) as a starting material instead of iodoacetophenone 1a (Fig. 1). Compound 2b was obtained in a yield of 31%. ^{1}H NMR ($CDCl_3$) δ, 7.75 (d, J=8.1 Hz, 2H), 7.59 (d, J=7.8 Hz, 2H), 6.43 (s, 1H). Product 2b was then reacted with 4-methylsulfonylphenylhydrazine hydrochloride to give BMTP 3b as a colorless solid in a yield of 78%. ^{1}H NMR ($CDCl_3$) δ, 7.97 (d, J=8.8 Hz, 2H), 7.54 (d, J=8.5 Hz, 2H), 7.53 (d, J=8.8 Hz, 2H), 7.11 (d, J=8.8 Hz, 2H), 6.79 (s, 1H), 3.07 (s, 3H). FAB-MS calcd for $C_{17}H_{12}BrF_3N_2O2S$ [MH^+]: m/z 445, found 445.

2.2.3. 5-(4-Iodophenyl)-1-[4-(aminosulfonyl)phenyl]-3-trifluoromethyl-1H-pyrazole (IATP)

This compound was synthesized by the same method as for IMTP, except that 4-aminosulfonylphenylhydrazine hydrochloride was used instead of 4-methylsulfonylphenylhydrazine hydrochloride (Fig. 1). The product 2a was reacted with 4-aminosulfonylphenylhydrazine hydrochloride to give IATP 3c as a colorless solid in a yield of 85%. ^{1}H NMR ($CDCl_3$) δ, 7.93 (d, J=8.5 Hz, 2H), 7.73 (d, J=8.5 Hz, 2H), 7.47 (d, J=8.5 Hz, 2H), 6.97 (d, J=8.5 Hz, 2H), 6.78 (s, 1H), 4.99 (s, 2H). FAB-MS calcd for $C_{16}H_{11}IF_3N_3O_2S$ [MH^+]: m/z 494, found 494.

2.2.4. 5-(4-Bromophenyl)-1-[4-(aminosulfonyl)phenyl]-3-trifluoromethyl-1H-pyrazole (BATP)

This compound was synthesized using the same method as for BMTP, except that 4-aminosulfonylphenylhydrazine hydrochloride was used instead of 4-methylsulfonylphenylhydrazine hydrochloride. The product 2b was reacted with 4-aminosulfonylphenylhydrazine hydrochloride to give BATP 3d as a colorless solid in a yield of 48%. ^{1}H NMR ($CDCl_3$) δ, 7.94 (d, J=8.5 Hz, 2H), 7.53 (d, J=8.3 Hz, 2H), 7.47 (d, J=8.5 Hz, 2H), 7.11 (d, J=8.3 Hz, 2H), 6.78 (s, 1H), 4.89 (s, 2H). FAB-MS calcd for $C_{16}H_{11}IF_3N_3O_2S$ [MH^+]: m/z 446, found 446.

2.3. Radiolabeling

The radioiodinated IMTP and IATP were obtained by a halogen exchange reaction with sodium ^{125}I-iodine according to the methods of Kiyono et al. [19]. Briefly, BMTP or BATP was added to a mixture of sodium ^{125}I-iodine, ammonium sulfate and copper (II) sulfate pentahydrate in water in a vial. The reaction mixture was heated for 2 h at 140°C. After cooling, the reaction mixture was filtered with a 0.22-μm filter (Ultrafree-MC 0.22-μm filter unit, Millipore, Benford, TX). The filtered solution was applied to a reverse-phase high-performance liquid chromatography (HPLC) column (Cosmosil 5C_{18}-AR-300 Packed Column, 250×10 mm id,

Nacalai Tesque, Kyoto, Japan) and eluted at a flow rate of 2.0 ml/min with 10 mM KH_2PO_4/acetonitrile=1:1 for the purification of ^{125}I-IMTP (R_t=54 min for BMTP, 64 min for IMTP) and 10 mM KH_2PO_4/acetonitrile=53:47 for that of IATP (R_t=58 min for BATP, 70 min for IATP).

The radiochemical purity of the labeled compound was determined by TLC and analytical HPLC. The TLC was performed on a silica gel plate, developed with AcOEt/hexane=1:2 (R_f=0.6 for IMTP and 0.4 for IATP). Analytical HPLC was performed on a 150×4.6-mm id Cosmosil AR-300 column (Nacalai Tesque, Kyoto, Japan) eluted at a flow rate of 1.0 ml/min with 10 mM KH_2PO_4/acetonitrile=1:1 for ^{125}I-IMTP (R_t=18.0 min) and 10 mM KH_2PO_4/acetonitrile=53:47 for ^{125}I-IATP (R_t=17.9 min).

2.4. COX inhibitory potency

Peroxidase inhibitory activities of IMTP and IATP were assessed by measuring the COX-catalyzed oxidation of *N,N,N',N'*-tetramethyl-*p*-phenylenediamine (TMPD) by hydrogen peroxide using a commercially available kit (Colorimetric COX Inhibitor Screening Assay Kit, Cayman Chemical). Briefly, 10 μl of ovine COX-1 or COX-2 solution was added to a 96-well plate with 150 μl of 0.1 mol/L Tris buffer at pH 8.0, 10 μl of heme solution in DMSO and 10 μl of the test compound (final concentration: 10^{-4}–10^{-9} mol/L). After 5 min of incubation at 25°C, 20 μL of TMPD and 20 μL of 1.1 mM arachidonic acid were added to the mixture. The oxidation of TMPD was monitored by measuring the absorbance of the mixture with a plate reader at 600 nm. SC-58125, meloxicam and indomethacin were used as reference compounds.

2.5. Animal experiments

Animal studies were conducted in accordance with institutional guidelines, and the experimental procedures were approved by the Kyoto University Animal Care Committee.

Biodistribution studies were performed on male Sprague-Dawley rats. ^{125}I-IMTP (74 kBq/rat) or ^{125}I-IATP (74 kBq/rat) was administered to rats under chloral hydrate anesthesia by tail vein injection. At appropriate time points after the administration, the rats were sacrificed by exsanguinations under chloral hydrate anesthesia. Blood and organs were excised and weighed, and the radioactivity was measured with an auto well gamma counter (ARC2000, Aloka, Tokyo, Japan).

Table 1
COX inhibitory potency and selectivity of IMTP, IATP and reference compounds

Compounds	IC_{50} (μM)		IC_{50} ratio (COX-1/COX-2)
	COX-1	COX-2	
IMTP	>100	5.16±2.83	>19
IATP	>100	8.20±1.43	>12
SC58125	>100	1.36±0.44	>73
Meloxicam[a]	>100	29.0	>3.5
Indomethacin[a]	0.08	11.9	0.007

Mean±S.D. of three independent experiments.
[a] Mean of two independent experiments.

Table 2
Biodistribution of ^{125}I-IMTP in rats (%dose/g tissue)

	Time after injection (min)			
	10	30	60	180
Blood	0.08±0.02	0.08±0.01	0.06±0.01	0.04±0.01
Plasma	0.12±0.03	0.12±0.01	0.09±0.01	0.06±0.01
Heart	0.49±0.11	0.50±0.05	0.38±0.06	0.23±0.04
Lung	0.48±0.14	0.42±0.08	0.34±0.04	0.28±0.05
Liver	1.59±0.29	1.53±0.27	1.02±0.15	0.59±0.11
Kidney	0.65±0.14	0.60±0.07	0.42±0.06	0.34±0.05
Pancreas	0.59±0.13	1.26±0.56	0.67±0.11	0.88±0.35
Spleen	0.28±0.06	0.27±0.05	0.23±0.07	0.15±0.04
Stomach	0.27±0.10	0.19±0.04	0.23±0.06	0.17±0.05
Intestine	0.27±0.06	0.38±0.20	0.27±0.04	0.25±0.05
Muscle	0.07±0.02	0.22±0.04	0.17±0.03	0.16±0.01
Thyroid	0.37±0.25	0.54±0.13	0.69±0.30	0.58±0.26
Brain	0.25±0.06	0.23±0.04	0.17±0.03	0.10±0.02
Brain/blood[a]	3.19±0.17	2.87±0.31	2.74±0.24	2.67±0.09

Mean±S.D. for four to five animals.
[a] Brain-to-blood ratio.

2.6. Distribution to blood cells

Distribution of ^{125}I-IATP and ^{125}I-IMTP to blood cells and the effects of several compounds on the distribution were measured by using rat whole blood. Acetazolamide and chlorthalidone were used as reference compounds for binding to carbonic anhydrase (CA), chlorpromazine for binding to the cellular membrane of red blood cells and phenothiazine for binding to hemoglobin. Heparinized whole blood from male Sprague-Dawley rats was pre-incubated at 37°C with gentle shaking for 5 min and then ^{125}I-IMTP (0.74 kBq) or ^{125}I-IATP (0.74 kBq) was added. After incubation at 37°C for 10 min, chlorpromazine, phenothiazine, acetazolamide or chlorthalidone was added in final concentrations of 10 to 300 μg/ml and then incubated at 37°C for 10 min. A small portion of the blood samples was counted in an auto well gamma counter (Cobra II Auto-

Table 3
Biodistribution of ^{125}I-IATP in rats (%dose/g tissue)

	Time after injection (min)			
	10	30	60	180
Blood	0.63±0.08	0.53±0.03	0.44±0.03	0.45±0.05
Plasma	0.14±0.02	0.12±0.01	0.11±0.01	0.10±0.01
Heart	0.86±0.12	0.62±0.03	0.57±0.03	0.56±0.03
Lung	0.77±0.06	0.58±0.03	0.53±0.05	0.55±0.04
Liver	1.89±0.28	1.31±0.14	1.13±0.12	1.15±0.15
Kidney	0.92±0.11	0.64±0.03	0.55±0.05	0.58±0.06
Pancreas	0.77±0.07	0.79±0.06	0.71±0.06	0.78±0.18
Spleen	0.58±0.07	0.44±0.03	0.39±0.03	0.36±0.02
Stomach	0.24±0.04	0.19±0.06	0.24±0.04	0.22±0.06
Intestine	0.26±0.04	0.29±0.04	0.32±0.07	0.36±0.04
Muscle	0.23±0.06	0.28±0.01	0.27±0.03	0.29±0.03
Thyroid	0.58±0.18	0.47±0.14	0.60±0.07	0.51±0.17
Brain	0.23±0.02	0.22±0.02	0.21±0.01	0.20±0.01
Brain/blood[a]	0.36±0.05	0.42±0.03	0.48±0.03	0.45±0.05

Mean±S.D. for five animals.
[a] Brain-to-blood ratio.

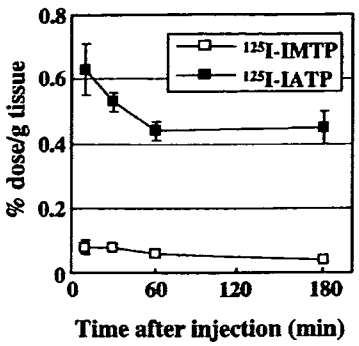

Fig. 2. Levels of ^{125}I-IMTP and ^{125}I-IATP in the blood. Mean±S.D. for four to five animals.

Gamma, Packard, Tokyo, Japan), and the rest were centrifuged for 1 min and the plasma separated. A small portion of the plasma samples was also counted. Hematocrit was measured using an i-STAT portable clinical analyzer (i-STAT, East Windsor, NJ). Distribution of the labeled compounds to blood cells was calculated as follows:

$$T = [1 - C_P/C_B \times (100 - H_t)/100] \times 100$$

where T is the distribution% to blood cells, C_P and C_B are the radioactivity in blood and plasma, respectively, and H_t is the hematocrit value.

2.7. Statistical analysis

Data are presented as mean values with the standard deviation, unless otherwise noted. Statistical analysis was performed by one-way ANOVA followed by Bonferroni–Dunn test for post hoc comparisons. Statistical significance was defined as a two-tailed P value <.05/6 (i.e., .0083).

3. Results

3.1. Synthesis and radiolabeling

IMTP, BMTP, IATP and BMTP were obtained with overall yields of 18%, 25%, 26% and 17%, respectively, from the starting material 1a or 1b. The radiosynthesis of ^{125}I-IMTP and ^{125}I-IATP was achieved with an iodine–bromide exchange reaction. ^{125}I-IMTP and ^{125}I-IATP were obtained with no carrier being added by the following separation from the precursors (BMTP and BATP) using reverse-phase HPLC. The radiochemical yields were 42% for ^{125}I-IMTP and 35% for ^{125}I-IATP, and the radiochemical purities were >95% for both of the labeled compounds.

3.2. COX inhibitory potency

IMTP and IATP inhibited COX-2 in a concentration-dependent manner, while they showed no inhibitory potency for COX-1 even at the highest concentration examined. Table 1 summarizes the IC_{50} values of the test compounds. The IC_{50} values of IMTP and IATP were 5.16 and 8.20 μM for COX-2 and >100 μM for COX-1. The COX-2 inhibitory potency of IMTP and IATP was higher than that of meloxicam (IC_{50}=29.0 μM) and comparable to that of SC-58125 (IC_{50}=1.36 μM). The IC_{50} ratio (COX-1/COX-2) for IMTP, IATP, SC-58125 and meloxicam was >19, 12, 73 and 3.5, indicating a high isoform selectivity of IMTP and IATP for COX-2.

3.3. Biodistribution

The biodistribution of ^{125}I-IMTP and ^{125}I-IATP is shown in Tables 2 and 3, respectively. The level of radioactivity for ^{125}I-IMTP in the blood decreased more rapidly than that for ^{125}I-IATP (Fig. 2). The radioactivity in the blood was 0.04 %dose/g tissue for ^{125}I-IMTP and 0.45 %dose/g tissue for ^{125}I-IMTP at 180 min after the tracer administration. At 10 min after the injection, high levels of the radioactivity were found in the liver and kidneys for both compounds. ^{125}I-IATP showed relatively higher levels of radioactivity in the heart and lung. Both compounds showed no marked accumulation in the stomach and thyroid. Significant levels of radioactivity were found in the brains of rats, with brain-to-blood ratios of 2.67–3.19 for ^{125}I-IMTP and 0.36–0.48 for ^{125}I-IATP.

3.4. Distribution to blood cells

Distribution of ^{125}I-IATP to blood cells (88.0%) was markedly higher than that of ^{125}I-IMTP (18.1%) as shown

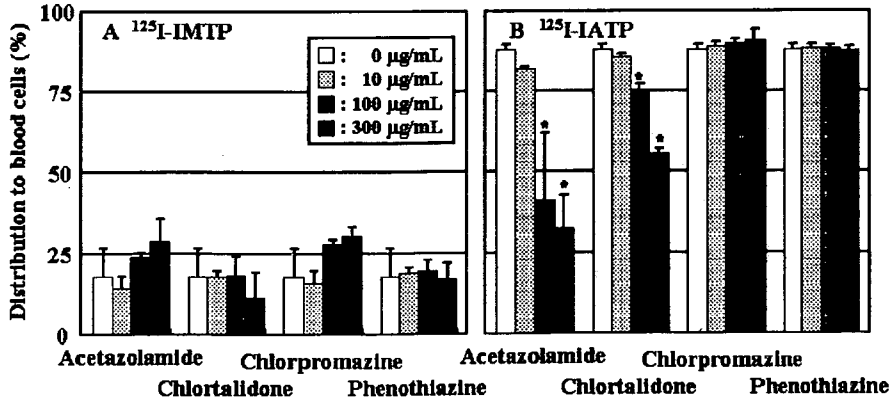

Fig. 3. Distribution of ^{125}I-IMTP (A) and ^{125}I-IATP (B) to blood cells. Mean±S.D. of three measurements. *P<.05/6 (i.e., .0083).